Proceedings of the ASME 2013 International Mechanical Engineering Congress and Exposition
IMECE2013
November 15-21, 2013, San Diego, CA, USA

IMECE2012-66416

OPTIMIZATION OF HYDROFOILS FOR HORINTAL AXIS MARINE CURRENT TURBINES USING GENETIC ALGORITHM

Krishnil R. Ram
The University of the South Pacific
Suva, Fiji

Jai N. Goundar
The University of the South Pacific
Suva, Fiji

Deepak Prasad
The University of the South Pacific
Suva, Fiji

Sunil Lal
The University of the South Pacific
Suva, Fiji

Mohammed Rafiuddin Ahmed
The University of the South Pacific
Suva, Fiji

ABSTRACT

As fossil fuels near depletion and their detrimental side effects become prominent on ecosystems, the world is searching for renewable sources of energy. Tidal energy is an emerging and promising renewable energy resource. Tidal turbines can extract energy from the flowing water in a similar way as wind turbines extract energy from the wind. The upside with tidal turbines is that the density of water is approximately 800 times greater than that of air and a tidal turbine harnessing the same amount of power as a wind turbine can be considerably smaller in size. At the heart of the horizontal axis marine current turbines are carefully designed hydrofoil sections. While there is a growing need to have hydrofoils that provide good hydrodynamic and structural performances, the hydrofoils also have to avoid cavitation for safe operation. This study uses a genetic algorithm optimization code to develop hydrofoils which have the desired qualities mentioned above. The hydrofoil problem is parameterized using a composite Bezier curve with two Bezier segments and 11 control points. Appropriate curvature conditions are implemented and geometric constraints are enforced to maintain the hydrofoil thickness between 16 to 18%. XFOIL is used as the flow solver in this study. The hydrofoils are optimized at Reynolds number of 2 million and for angles between 4 to 10 degrees. The best foil from the results, named USPT4 is tested for performance with the CFD code ANSYS CFX. The CFX results are validated with experimental results in a wind tunnel at the same Reynolds number. The hydrofoil's performance is also compared with a commonly used NACA foil.

INTRODUCTION

The electricity requirements around the globe are met mainly by burning huge quantities of fossil fuel [1]. The continuous increase in the fossil fuel price and environmental related problems caused by burning fossil fuel is now a global issue [2]. On the other hand, the demand of electricity keeps increasing, due to increase in world population, increase in industrialization and industries becoming manual to automated, the demand for electricity is predicted to double by 2053 compared to that in 2008 [3]. This has challenged researchers to look for alternative energy sources; renewable energy is becoming favorable alternative energy source for fossil fuels. Many renewable energy technologies have been exploited over the years, the drawback of renewable energy technology is that limitation of resources available at one location, and it is not viable to store it for longer period of time, therefore, electrical energy from number of sources will be required to feed in to the grid.

Marine current energy is a clean and reliable source of renewable energy; it is one of the alternative energy sources

for fossil fuels. Horizontal axis marine current turbines (HAMCT) can be used to generate electricity for commercial use for any location where the marine current velocity exceeds 2 m/s [4]. Developments have taken place globally on HAMCT over the years from improvement in the efficiency of models to prototype building and installation. Works of Bahaj et al. [5, 6] involve developing, designing and model testing of bi-directional marine current turbines. Hwang et al. [7] designed HAMCT with improved efficiency by developing and designing individual blades with control. CFD method has been developed and now being used to compute and analyze 3D HAMCT performance [8-10]. Sale et al. [11] optimized the twist and chord distribution of HAMCT blades using genetic algorithm (computation code); this is developing to be an effective method for optimizing turbine blades with improved hydrodynamic performance. These turbines yield the maximum efficiency between 45-48%. Another effective method of improving the turbine performance is by placing a duct around the turbine - RTT by Lunar Energy [12], SeaGen by Marine Current Turbines (MCT) [13], some early investigations and testing performed by Thorpe [14] and Clean Current's tidal turbine [15]. Placing the shroud/duct will increase the cost; therefore the increase in efficiency must be significantly higher to justify the higher turbine cost. Whether it is a shrouded or a non-shrouded turbine, the blade sections (hydrofoils) needs to be very carefully designed so that it can operate over a wide range of conditions, and should be structurally strong to withstand strong hydrodynamic forces. For most cases, airfoils are directly used as hydrofoils, but this results in a higher chance of cavitation inception; using modified airfoils as hydrofoils results in delayed cavitation inception [4, 16]. A useful method to optimize airfoil/hydrofoil geometry for specific turbine applications is using Genetic Algorithm (GA) code [11, 17-22].

HAMCT is governed by lift, and the design and operating concept is similar to Horizontal axis wind turbine (HAWT) [23]. Hydrofoils are the blade sections and play a very important role in overall performance of HAMCT. For a successful design of hydrofoils, it requires one to study detailed hydrodynamic characteristics of hydrofoils. Hydrofoils operates in a similar way as airfoils, generating lift force as the fluid passes over the surface, but there are some fundamental differences in the design and operation of hydrofoils. These are very high Re, and strong hydrodynamic forces on hydrofoil (requiring thick hydrofoils); the main challenge in designing hydrofoils is occurrence of cavitation, useful information on cavitation and the stall characteristics of marine propellers is available and can be utilized in hydrofoil design [24]. Once cavitation inception is predicted at 2D design stage, then we can move ahead and analyze rotor performance with 3D analysis.

In the current study, a hydrofoil has been optimized for the tip region of the blade using a GA code. For seeding, foil SG6043 was used after carefully studying its hydrodynamic characteristics. The generated hydrofoil is named as USPT4, it has a maximum thickness of 17%, and has lower suction peak over a wide range of α. The hydrofoil also has high L/D ratios for α between 4-10 degrees.

OPERATING CONDITIONS AND DESIGN PARAMETERS

The important hydrofoil characteristics that need to be studied when designing are C_{Pmin} and L/D ratio. A good hydrofoil must have a high L/D ratio over a wide range of α with delayed stall, and lower suction peak on the upper surface of the hydrofoil to prevent cavitation. For the case of HAMCT, the blade sections needs to be thick, so that the blade can withstand large hydrodynamic forces. For hydrofoil design stage, the 2D panel method XFoil can be used [4]. XFoil is a linear vorticity stream function panel method with viscous boundary layer and wake model, and is found to be a suitable tool for predicting cavitation criteria and hydrofoil characteristics at the preliminary design stage [25]. It is very important to avoid cavitation on the blade's surface. Cavitation causes structural damage and adversely affects the turbine's performance; the pressure associated with bubble collapse is high enough to cause failure of metals [26]. Cavitation inception occurs when the minimum local pressure on the blade surface falls below the vapour pressure of the fluid. Cavitation inception can be predicted by comparing the local minimum C_P with the cavitation number σ [4]. Hydrofoil will encounter cavitation if the C_{Pmin} is lower than $-\sigma$ or C_{Pmin} is lower than C_{Pcrit} ($C_{Pcrit} = -\sigma$). The cavitation number is defined as

$$\sigma = \frac{p_O - p_V}{0.5\rho W^2} = \frac{P_{AT} + \rho g h - p_V}{0.5\rho W^2} \quad (1)$$

The risk of occurrence of cavitation is higher on the blade towards the tip due to low immersion depth near the tip and the highest relative velocity experienced near the tip. An important parameter in predicting cavitation on hydrofoil is its Re – information of turbine geometry and turbine operating conditions are required for calculating Re. Mostly 3-bladed HAMCT are used, 3-bladed turbines has less vibrations during operation and the marine streams are not usually wide and deep, therefore, the turbine size is limited to 10-15 m, the rated speed was set to be 2 m/s and TSR (Tip Speed Ratio) of

4; the Re comes to around 2 million near the tip of the turbine. To predict cavitation, C_{Pcrit} was determined at different locations on the blade using the above-mentioned geometric and operating conditions. The C_{PCrit} at the blade location (r/R) of 0.6 to 1.0 and for tidal current velocities of 2 m/s, 2.5 m/s and 3 m/s are shown in Fig. 1.

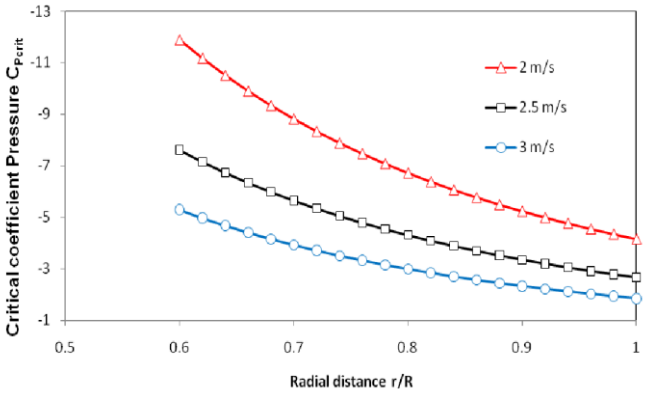

Figure 1. Variation of the critical pressure coefficient along the blade for different current velocities.

The C_{pcrit} for blade tip at tidal current velocities of 1 m/s and 1.5 m/s are around -16 and -8 (not shown), therefore, the chances of cavitation are almost zero at these velocities. As the velocity increases above 2 m/s, the chances of cavitation increase at r/R of 0.6 to 1.0. The cavitation may occur on the outer 10% of the blade if the C_{Pmin} drops below -4.0, -2.7, and -1.8 for velocities of 2 m/s, 2.5 m/s and 3 m/s respectively. For these cases, it is necessary to pitch the blade to avoid cavitation.

OBJECTIVE FUNCTIONS

The objective of the algorithm is to maximize the lift while minimizing or fixing the drag and keeping the thickness between 16 to 18% of the chord. After many experiments with the optimization algorithms, it was found that improving the performance at multiple angles such as from 4° to 10° is computationally expensive. However, optimizing at the minimum and maximum angles also has the effect of causing nearby angles to be optimized as the lift and drag curves follow a smooth function. For this reason, the hydrofoil was optimized at angles of 4° and 10°. The objective function was built as follows:

1. Minimize drag coefficient (C_d), Maximize lift coefficient (C_l) for α_i ..... α_n.
2. Keep Cp below critical value. (constraint).

This gives the following generalized fitness function:

$$F(B(u),\mathrm{Re}) = \sum_{i=1}^{n}\left(\frac{Cl_i}{Cd_i * 1.1}\right)\times\frac{1}{m} \qquad (2)$$

where m is the number of angles which is 2 for this case. For this case α_1 = 4° and α_2 = 10°. The Reynolds number (Re) chosen for optimization was 2 million as this is common for tip regions of tidal turbines in average streams of 2.5 m/s. The Bezier curve function is discussed in detail in later sections. To get a much better idea of only leading edge transition effects on the optimization method, the free-stream turbulence intensity was set to 2.981%.

HYDROFOIL PARAMETERIZATION AND OPTIMIZATION PROCEDURE

Before optimization can be applied to a problem, it needs to be defined as a mathematical model taking into account all the variables and parameters. In order to optimize the hydrofoil, the 2D shape of the hydrofoil needs to be parameterized by defining the variables that will control the coordinates and shape of the hydrofoil. In this study, the need was for a single discipline shape parameterization scheme whereby only the shape function will be parameterized. It was essential to carry out a study of existing parameterization methods. This is discussed in detail in ref. [27]. One of the most common and easiest ways to represent free form curves is via Bezier curves. Bezier curves were developed by Paul de Faget de Casteljau [28] and later popularized by Pierre Bezier. Bezier curve parameterization allows the use of a parameter u, and multiple control points $\boldsymbol{P}_i$ to generate x and y coordinates of an airfoil. This study makes use of Bezier curves to parameterize the airfoil. Several studies [17, 19] have used Bezier airfoil parameterization for airfoil optimization. The Bezier parameterization scheme is easy to implement along with constraints and has reasonable accuracy. The parameterization uses control points outside the airfoil curve as parameters. The following paragraph details the parameterization method.

Bezier curve parameterization allows the use of a parameter u, and multiple control points $\boldsymbol{P}_i$ to generate x and y coordinates of an airfoil. This study makes use of Bezier curves to parameterize the airfoil. The Bezier parameterization scheme is easy to implement along with constraints and has reasonable accuracy. The order of the Bezier curve is determined by the number of control points. For $n + 1$ control points $\boldsymbol{P}i$, a Bezier curve of the nth order will be formed. By joining the control points together, a control polygon is formed. The generalized form of a Bezier curve is defined as:

$$\mathbf{B}(u) = \sum_{i=0}^{n} \mathbf{P}_i \frac{n!}{i!(n-i)!} u^i (1-u)^{n-i} \quad , u \in (0,1) \qquad (3)$$

where ***B*** *(u)* vector contains the x and y coordinates on the curve and $\boldsymbol{P}_i$ contains the x, y coordinates of the control polygon. The parameter *u* is defined from 0 to 1 uniformly in this study. For this study a composite Bezier curve was used to define the geometry of the hydrofoil. One Bezier curve was used to represent the upper surface while a second Bezier curve was used to represent the lower surface as shown in Figure 2.

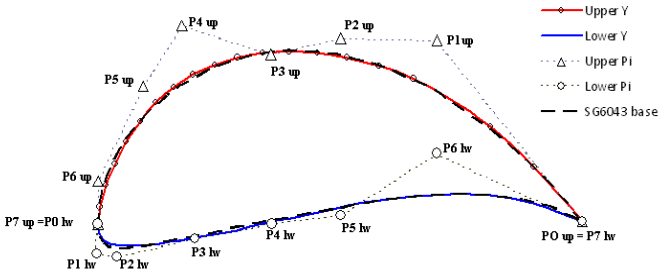

Figure 2. Bezier curve parameterization of SG6043(6) foil using composite Bezier curves , *up* = upper surface, *lw* = lower surface. Points *P* were achieved through interpolation.

The start and end control points, *PO* and *P7* lie on the foil curve itself at the leading and trailing edges and their positions are fixed to maintain a chord length of unity for easier computation and comparison in the flow solver XFOIL. Specific conditions were defined to control the integrity of the airfoil shape at the leading and trailing edge. At the leading edge the initial and terminal points of the upper and lower curves coincide to close the curve. C^0 continuity is enforced at the trailing edge by simply connecting the upper and lower curve points without any special condition. At the leading edge, C1 continuity was enforced by ensuring that *P1 lw* is a reflection of *P6 up* with the mirror line being perpendicular to segment *P1 lw – P6 up* and crossing at *P7 up*. Despite the leading and trailing edges being fixed, the upper and lower surfaces of the foil had a large degree of freedom and has the possibility to represent a suitably large number of free form closed shapes. With the leading and trailing points restricted and *P1 lw* being governed by the coordinates of *P6 up*, a total of 11 control points were available to manipulate the airfoil shape. Higher order (10^{th}) curves were also experimented on but these increased the number of control points and were prone to form bumps due to enhanced local control which was not taken well by the geometry-sensitive solver. The 7^{th} order Bezier foil parameterization function was coded in C++. Geometric constraints on the foil ensured that only realistic hydrofoil shapes were analyzed. The constraints are described later in the paper.

The problem of increasing lift and other favorable characteristics of hydrofoil while minimizing or maintaining drag and other unwanted traits calls for a suitable multi – objective optimization scheme. In this case, the L/D needs to be improved within a given thickness value. The Genetic Algorithm (GA) optimization approach was developed by Holland [29] and has seen use in numerous optimization problems owing to its robust approach. The GA is a stochastic algorithm and it keeps in memory a population of solutions during iteration rather than a single solution. The GA uses a direct analogy of natural behavior. While conventional GA represents the population of solutions in binary bits, recent developments have allowed for real valued GA approach. The solutions of GA are coded as an array of bits called chromosomes or genotype. The genotype represents an individual in a solution vector called the phenotype. GA is an iterative process and each iteration is called a generation. The initial population is made up of individual solutions represented in chromosomes. Each individual is subjected to a fitness function that will determine its fitness values. Normally the chromosomes with the desired or closer to desired fitness values are chosen to be parents in the next generation. During selection it is common to use a roulette wheel. Here the selection is made biased by assigning better solution a higher probability of getting selected. The parents are then mated using crossover methods to form the next population set. Mutations are allowed to avoid solutions getting stuck in local maxima. The fitness function is repeated on the next set of population until a termination condition is reached. The termination condition may be reached if a satisfactory solution is found or at the end of the generations. This study utilizes the binary coded GA written in C++ by Lal et al. [30].

Figure 3 shows the flow of information in the GA optimization. Initialization of the population also includes seeding of the popular SG6043 airfoil control points. Seeding an airfoil shape into the GA code provides the code some idea of a good airfoil and it does not have to start from an abstract shape altogether. Since GA optimizes the control points of the Bezier functions that govern the foil shapes, the 11 control points were discretized into a bit string of 88 bits with each control point represented using 8 bits.

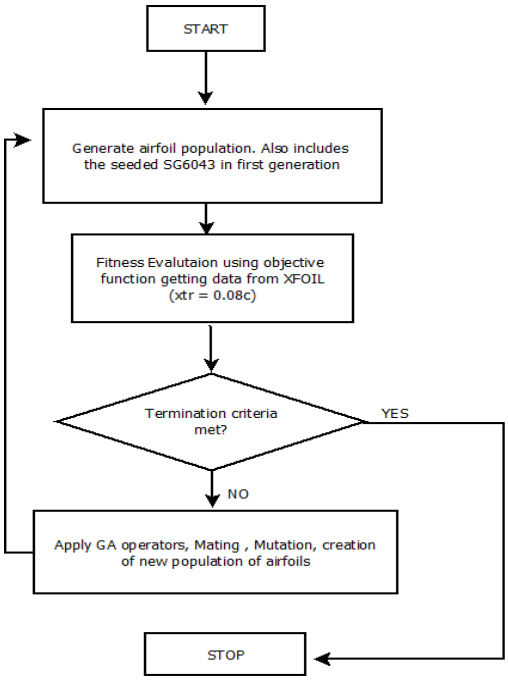

Figure 3. Flowchart for hydrofoil optimization using GA.

GEOMETRIC CONSTRAINTS AND FITNESS EVALUATION

The flow solver used in this study is highly sensitive to geometry and hence strict geometry conditions are set to prevent unnecessary analysis and failure of analysis by passing nonrealistic hydrofoil shapes to the solver.

To ensure that the upper and lower Bezier curves do not overlap, the following condition was set.

$$Y(u)_{upper} - Y(u)_{lower} > 0 \text{ , (Except for } P0 \text{ and } P7) \quad (4)$$

To maintain structural strength of the blade, the blade section must be sufficiently thick. The thickness is maintained between 16 to 18% of the chord at the tip using the following condition.

$$0.16c > (Y(u)_{upper} - Y(u)_{lower}) > 0.18c \quad (5)$$

The upper and lower limit of the y coordinates was set to prevent highly cambered airfoils and to maintain a realistic search space. The x coordinates were fixed in order to reduce the number of control variables.

$$(Y(u)_{upper}) \leq 0.2 \qquad (Y(u)_{lower}) \geq -0.1 \quad (6)$$

Instead of coding the constraints along with the individual solutions, the solutions are allowed to override these conditions initially. Once the shapes are created, a pre- fitness evaluation is done and the shapes that are not conforming to any of the geometric conditions are assigned the lowest fitness value of 1 and further analysis of these curves is not permitted. The popular panel method viscous/inviscid flow solver XFOIL [25] was used to calculate the C_l and C_d values of the hydrofoils at pre-defined Reynolds numbers and α. The C_l and C_d values were input to the fitness function (Equation 2).

EXPERIMENTAL AND CFD ANALYSIS

Numerical analysis was performed on the USPT4 hydrofoil using ANSYS ICEM-CFD and CFX software. Flow over hydrofoils was analyzed for different α and Re values. A hexahedral mesh based on O-grid and C-grid topology was created around the foil with 300,000 nodes. The mesh density was increased near the leading and trailing edges to capture the peak suction, stagnation and transition points. A *k-ω* shear stress and transport turbulence model was used. The hydrofoil was also tested in XFOIL from 0 to 15 degrees. Essential characteristics such as C_l, and C_d were noted and compared with experimental results. An open circuit, suction type low speed wind tunnel was used. The Engineering Laboratory Design (ELD) Inc wind tunnel in the Fluids laboratory at the University of the South Pacific with speed range from 3 m/s to 49 m/s was used. A centrifugal fan powered by a 10 HP AC 3-phase thyristor controlled motor is used to generate the airflow. A maximum velocity resolution of 0.08 m/s is achievable in the test section. The test section measures 305 mm x 303 mm x 1000 mm. A traversing pitot-static tube was used to measure the velocity in the wind tunnel test section. A Furness Controls FCO510 digital micro-manometer was used to take pressure readings. The USPT4 profile was milled out of wood and 22 pressure taps were provided on the upper surface and 13 on the lower surface. The USPT4 foil was polished to ensure a smooth surface. The foil was fixed from wall to wall to avoid 3-dimensional flow effects in the experiment. The pressure taps were placed near the middle of the test section, which ensured that any effect of the test section boundary layer is not felt by the pressure taps. A separate section of the foil was milled and finished without any pressure taps. This was for direct lift (L) and drag (D) force measurements. A two component lift and drag dynamometer equipped with a Linear Variable Differential Transformer (LVDT) was used. The dynamometer has an accuracy of 1 g(f). The hydrofoil was tested at a Reynolds number of 250,000 and the results were compared with numerical results.

RESULTS

The results of XFOIL, experimental and CFD tests are presented in this section. The profile of USPT4 is compared with that of NACA63-814 in Fig. 4. Both foils have the same thickness of 17% of the chord. The USPT4 was generated to

maintain a thickness between 16% to 18%, as mentioned earlier.

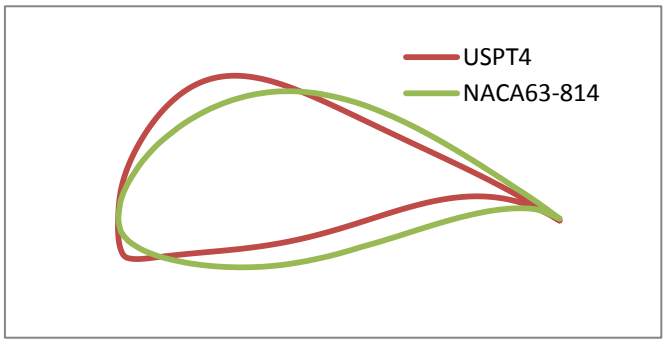

Figure 4. Hydrofoil USPT4 compared to the NACA63-814 tidal turbine hydrofoil (not to scale).

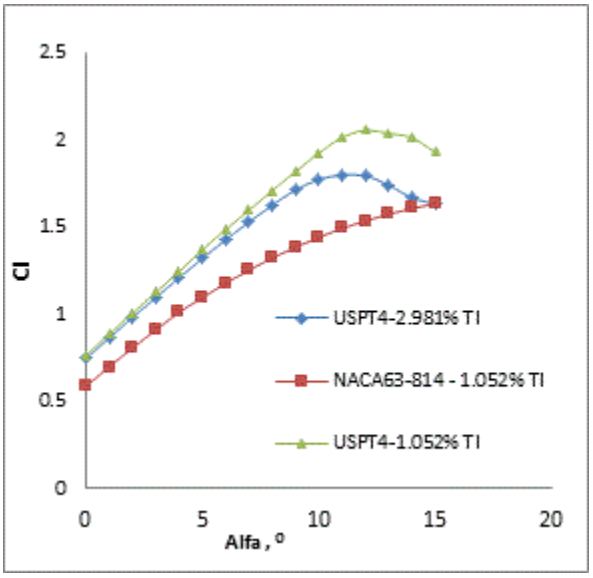

Figure 5. Lift coefficient of the two hydrofoils at Re = 2 million.

Figure 5 shows the lift coefficient of the hydrofoils at different angles of attack. The USPT4 stalls at around 11 degrees when turbulence intensity is around 1% and at 12 degrees for 2.98% turbulence intensity. The USPT4 has higher lift coefficents in both the cases compare to NACA63-814. Stall occurs softly so there will not be any abrupt change in power production if there is any change in the flow direction. Since the tip region generates most of the lift, strength is not a major issue here and high C_l values are advantageous.

Figure 6 shows the drag polars for the USPT4 and NACA foils. Drag polars are useful in determining the relation between lift and drag coefficients. While lift keeps increasing until the stall angle, drag also rises. The operating point is located from the drag polar such that maximum lift is attained when the drag is still small.

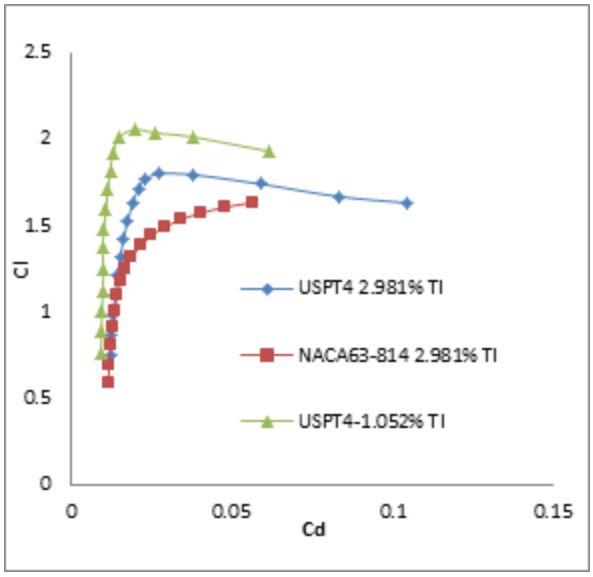

Figure 6. Drag polars for the two hydrofoils at 2 million Reynolds number.

In the case of USPT4, a good operating angle is apparently 10 degrees. This corresponds to C_l of 1.77 and C_d of 0.023. The operating angle is determined at the higher turbulence of 2.98%.

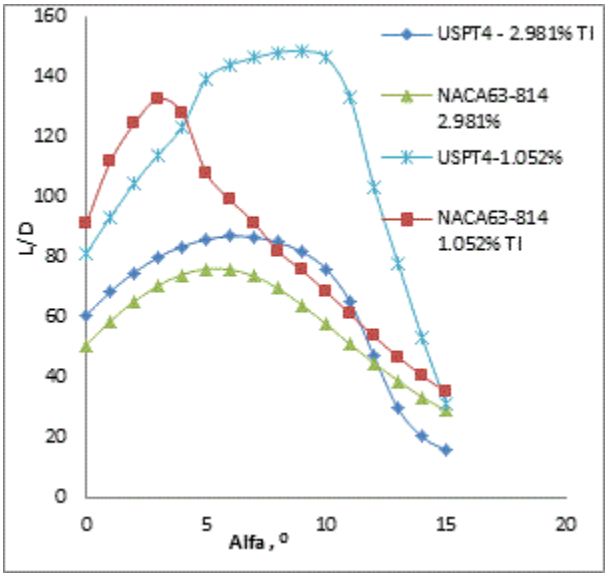

Figure 7. Lift-to-drag ratio of the hydrofoils at Re = 2 million at different turbulence intensities.

The tip region of the blade is expected to contribute a lot more to power production compared to the inboard regions of the blade. For this reason, the efficiency or the lift to drag ratio has to be considerably high for the hydrofoil. Figure 7 shows that USPT4 has reasonably good L/D at the Reynolds number of 2 million. Since lift increases at higher angles, the corresponding operating points are preferred to be at high angles. At the turbulence intensity of 1.052%, the USPT4

hydrofoil peaks at 9 degrees with L/D reaching 148 and drops off from 10 degrees onwards. The NACA63-814 has maximum L/D of 127 at 3 degrees. While L/D may be high, if this L/D occurs at low angles of attack, this may not be as useful as higher L/D at higher angles of attack. As turbulence increases to 2.98%, the USPT4 is affected and a drop in L/D takes place for all angles. The turbulence increases frictional drag and reduces the L/D ratio. However, peak L/D drops to 86 at 7 degrees. It may be suitable to choose an operating point around 7 degrees so that slight change in angle of attack will not adversely affect the performance even in case of high turbulence which is common in tidal streams. L/D at higher turbulence intensities is still higher than the NACA63-814 foil. Despite being of the same thickness, the USPT4 outperforms the NACA63-814 in terms of hydrodynamics.

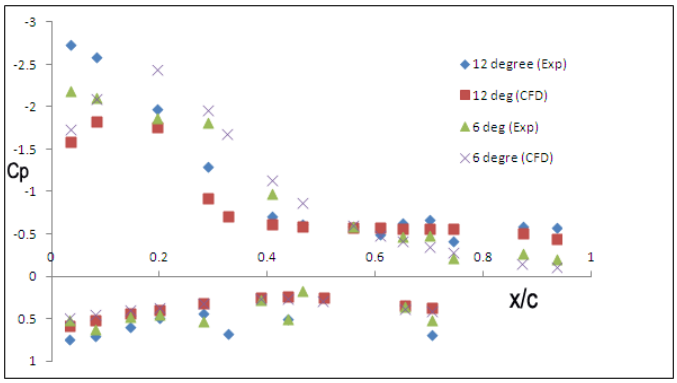

Figure 8. Experimental and Numerical Coefficient of pressure at Reynolds number of 220,000.

Figure 8 shows the coefficient of pressure measured on the upper and lower surface of the hydrofoil at Re= 220k. The measurement results are in reasonably good agreement with CFX results except for the upper surface locations close to the leading edge.

Figure 9 shows the minimum Cp that occurs at each angle of attack. From previous calculations, it was found that the Cp required for the onset of cavitaion is around -4.11 for a chord of 250 mm with free-stream velocity of 2 m/s. It is evident from Fig. 9 that while Cp values reach a minimum of -4.1 at 14 degrees, this is not of concern in the design. This is because this angle is out of the normal operating angle range of the hydrofoil. Even at low turbulence intensity, the hydrofoil USPT4 will stall at around 12 degrees. The stall would apparently slow down or stop the turbine's rotation and hence the conditions that will cause a Cp 0f -4.1 will not likely occur. The least Cp experienced in design situation is -3.77 which is safe from the cavitaion Cp of -4.11 in this case.

Figure 10 shows the pressure contours around the hydrofoil at Re = 2 million for the angle of attack of 6^o. The stagnation point occurs on the lower surface of the hydrofoil. The build-up of high pressure on the lower surface and the suction on the upper surface can be seen.

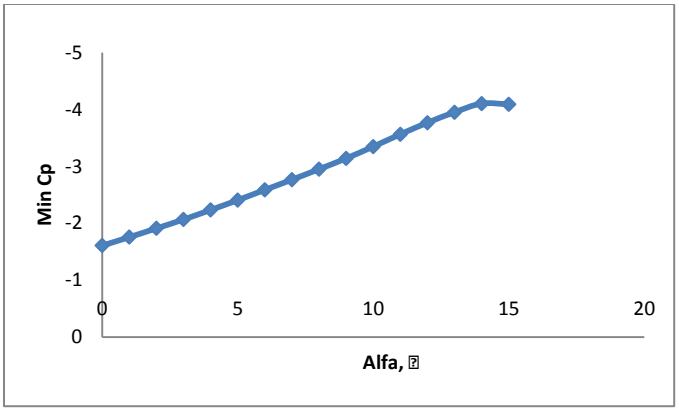

Figure 9. Minimum Cp for each angle of attack at Re = 2 million and turbulence intensity of 1.052%.

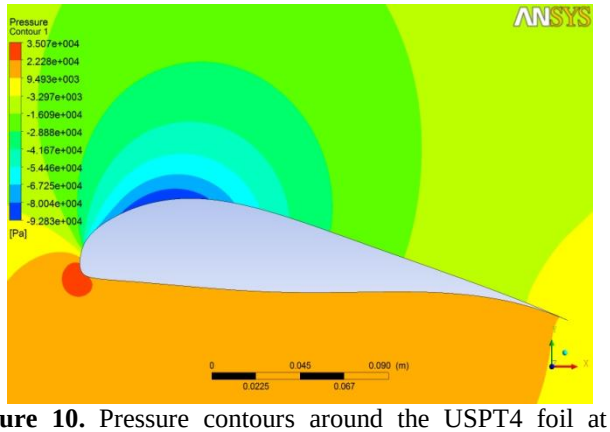

Figure 10. Pressure contours around the USPT4 foil at 6 degrees and Re = 2 million

Figure 11 shows the streamlines around the foil at an angle of attack of 12^o and Re = 2 million. While there is a strong suction on the upper surface with the maximum velocity nearly double of the free-stream velocity, the flow separation from the upper surface due to the adverse pressure gradient (shown in Fig. 8) can clearly be seen from this figure.

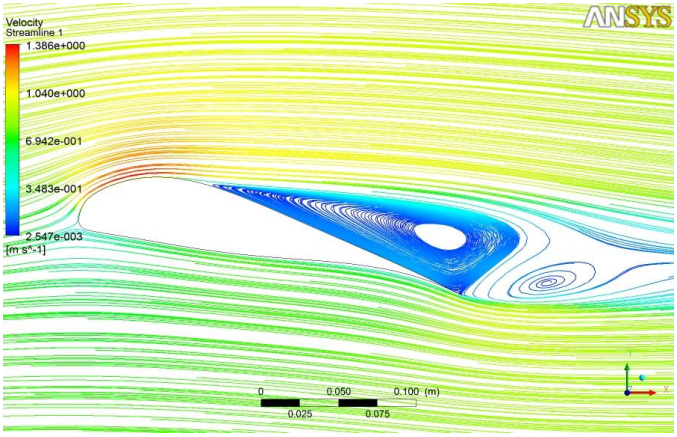

Figure 11. Streamlines around the USPT4 foil at 12 degrees and Re = 2 million.

CONCLUSIONS

A hydrofoil suitable for the tip region of a tidal current turbine is designed and tested for performance. Unlike wind turbines, care must be taken to avoid cavitation on tidal turbine blades. For this reason, the minimum Cp was kept well below the cavitation limit for a relative velocity of 6 m/s. The USPT4 has been designed using genetic algorithm optimization and while it has suitable thickness of 17%, it also has good hydrodynamic characteristics with L/D ratios as high as 148 at higher angles of attack. Over the range of angles of attack of 6^o to 12^o, the performance of the foil will not deteriorate, resulting in good output from the turbine.

REFRENCES

[1] Rourke, F.O., Boyle, F., Reynolds, A., 2010, "Tidal Energy update 2009," *Applied Energy*, 87: 398-409.

[2] Charlier, R.H., 2003, "A "Sleeper" awakes: tidal current power," *Renewable and Sustainable Energy Reviews*, 7(3): 187-213.

[3] Davood, S., Ahmad, S., Pourya, A., Ali A.A., 2013, "Aerodynamic design and economical evaluation of site-specific small vertical axis wind turbines," *Applied Energy*, 101: 765-775.

[4] Batten, W.M.J., Bahaj, A.S., Molland, A.F., Chaplin, J.R., 2006, "Hydrodynamics of marine current turbine," *Renewable Energy*, 31: 249-56.

[5] Bahaj, A.S., Molland, A.F., Chaplin, J.R., Batten, W.M.J., 2006, "Power and Thrust measurement of marine current turbines under various hydrodynamic flow conditions in a cavitation tunnel and a towing tank," *Renewable Energy*, 32: 407-426.

[6] Batten, W.M.J., Bahaj, A.S., Molland, A.F., Chaplin, J.R., 2006, "The prediction of Hydrodynamic performance of marine current turbines," *Renewable Energy*, 33: 1085-96.

[7] Hwang, I.S., Lee, Y.H., Kim, S.J., 2009, "Optimization of cycloidal water turbine and the performance improvement by individual blade control," *Applied Energy*, 86:1532–1540.

[8] Lee, J.H., Park, S., Kim, D.H., Rhee, S.H., Kim, M.C., 2012, "Computational methods for performance analysis of horizontal axis tidal stream turbines," *Applied Energy*, 98: 512-523.

[9] Kinnas, S.A., Xu W., 2009, "Analysis of tidal turbines with various numerical methods," Proceedings, 1st annual MREC technical conference, MA, USA.

[10] Harrison, M.E., Batten, W.M.J., Myers, L.E., Bahaj, A.S., 2009, "A comparison between CFD simulations and experiments for predicting the far wake of horizontal axis tidal turbines," *Proceedings, 8th European wave and tidal energy conference*, Uppsala (Sweden).

[11] Sale, D., Jolman, J., Musial, W., 2009, "Hydrodynamic optimization method and design code for stall-regulated hydrokinetic turbine rotor," National Renewable energy laboratory.

[12] Jones, J.A., Chao, Y., 2009, "Offshore hydrokinetic energy conversion for onshore power generation," *Proceedings, ASME 2009 28th international conference on ocean, offshore and arctic engineering (OMAE2009)*, Honolulu, Hawaii, USA.

[13] Fraenkel, P., 2010, "Development and testing of marine current turbine's SeaGen 1.2MW tidal stream turbine," *Proceedings, International conference on ocean energy, ICOE 2010*, Bilbao, Spain.

[14] Thorpe, T., 2005, "The advantages of ducted over unducted turbines," *Proceedings, 6th European wave and tidal energy conference*, pp. 523–528.

[15] Niet, T., McLean, G., 2001, "Race rocks sustainable energy development," *Proceedings, 11th Canadian hydrographic conference*, Victoria, British Columbia.

[16] Goundar, J.N., Ahmed, M.R., Lee, Y.H., 2012, "Numerical and experimental studies on hydrofoils for marine current turbines," *Renewable Energy*, 42: 173–179.

[17] Grasso, F., 2010, "Usage of Numerical Optimization in Wind Turbine Airfoil Design," *Proceedings, 28th AIAA Applied Aerodynamics Conference - Aerodynamics Design: Analysis, Methodologies & Optimization Techniques*, Chicago, USA.

[18] Quagliarella, D., and Vicini, A., 2001, "Viscous Single and Multicomponent Airfoil Design with Genetic Algorithms," *Finite Elements in Analysis and Design*, 37**,** 365-380.

[19] Gardner, B. A., and Selig, M. S., "Airfoil Design Using Genetic Algorithm and an Inverse Method," *Proceedings, 41st Aerospace Sciences Meeting and Exhibit*, Reno, Nevada, USA.

[20] Samareh, J. A., "A Survey of Shape Parameterization Techniques," *Proceedings, CEA/AIAA/ICASE/NASA Langley International Forum on Aeroelasticity and Structural Dynamics*, Williamsburg, VA, 333-343.

[21] Defalco, I., Balio, R. D., Cioppa, A. D., and Tarantino, E., 1995, "A Parallel Genetic Algorithm for Transonic Airfoil

Optimisation," *Proceedings, IEEE International Conference on Evolutionary Computation*.

[22] Kharal, A., and Saleem, A., 2012, "Neural Networks Based Airfoil Generation for a Given Cp Using Bezier–Parsec Parameterization," *Aerospace Science and Technology*, 23: 330-344.

[23] Burton, T., Sharpe, D., Jenkins, N., Bossanyi, E., 2000, *Wind energy handbook*. Wiley.

[24] Carlton, J, S., 1994, Marine propellers and Propultion. Butterwworth Heinemann.

[25] Drela M., 1989, "XFoil: an analysis and design system for low Reynolds number airfoils," *Proceedings, Conference on low Reynolds number airfoil aerodynamics*, University of Notre Dame; 1989.

[26] Eisenberg, P., 1950, *Mechanics of cavitation*, Hydronautics incorporated.

[27] Ram, K., Lal, S. and Ahmed, M. R., 2012, "Airfoil Optimization for Small Wind Turbines Using Multi-Objective Genetic Algorithm," *Proceedings, ASME 2012 International Mechanical Engineering Congress and Exposition*, Houston, USA, *ASME Paper No. IMECE-2012-88788*.

[28] Bieri, H. P., and Prautzsch, H., 1999, "Preface," *Computer Aided Design and Geometry*, 16; 579-581.

[29] Holland, J. H., 1975, *Adaptation in Natural and Artificial Systems*, University of Michigan Press.

[30] Lal, S., Yamada, K., and Endo, S., 2008, *Emergent Motion Characteristics of a Modular Robot through Genetic Algorithm,Advanced Intelligent Computing Theories and Applications With Aspects of Artificial Intelligence*," Springer Berlin / Heidelberg.